

# Persistent Current States in Bilayer Graphene

Jeil Jung,<sup>1</sup> Marco Polini,<sup>2</sup> and A.H. MacDonald<sup>1</sup>

<sup>1</sup>*Department of Physics, University of Texas at Austin, Austin, Texas 78712, USA*

<sup>2</sup>*NEST, Istituto Nanoscienze-CNR and Scuola Normale Superiore, I-56126 Pisa, Italy*

Broken symmetry states that carry equilibrium currents were proposed some time ago by researchers seeking a microscopic theory of superconductivity, but have never been observed. In this Letter we point out that the unusual electronic structure of unbalanced bilayer graphene is particularly favorable for the realization of this interesting type of ordered state.

The search for a microscopic theory of superconductivity, ultimately brought to a conclusion by the successful work of Bardeen, Cooper, and Schrieffer [1], led a number of early condensed matter theory researchers [2–4] to speculate on the possibility that interactions could under some circumstances lead to electronic states that carry currents in equilibrium. Such a state would have to break rotational and time-reversal symmetry. From a more modern point of view, its continuous formation would be signaled by an angular momentum  $\ell = 1$  charge-channel Pomeranchuk [5] (Fermi-surface distortion) instability.

An  $\ell = 1$  Fermi-surface distortion transfers occupation between quasiparticle states with opposite current components along the continuously variable direction in which overall current flows, as illustrated schematically in Fig. 1. For a translationally-invariant electronic system, however, it is known from both microscopic-quantum-mechanical [6, 7] and Fermi-liquid-theory [8] points of view that such a distortion corresponds simply to a Galilean boost which raises the center-of-mass kinetic energy and does not change the interaction energy. An  $\ell = 1$  charge-channel Pomeranchuk instability is therefore an impossibility in an electron fluid. In a crystal, where the Pomeranchuk instability notion refers to Fermi-surface distortions which reduce lattice symmetries,  $\ell = 1$  distortions have also been viewed [9] as extremely unlikely. Instabilities with  $\ell = 2$ , which lead to electron nematic states, do on the other hand appear to occur [10, 11] in a variety of different systems and spin-channel  $\ell = 0$  instabilities, which lead to ferromagnetism, are common. In this Letter we point out that a Bernal-stacked graphene bilayer (BLG) in which a gap has been opened by a transverse electric field is ideally suited to host an  $\ell = 1$  Pomeranchuk instability because its electron and hole Fermi seas are disks that are spread widely over momentum space, as illustrated in Fig. 1(b) [12]. Fermi-surface distortions with  $\ell = 1$  can lower energy by compactifying the Fermi sea to realize the momentum-space condensation envisaged by London [4] more than seventy years ago.

Recent progress [13] has made it possible to prepare and study the electronic properties of two-dimensional (2D) electron systems based on single- and few-layer graphene. This advance has provided researchers with

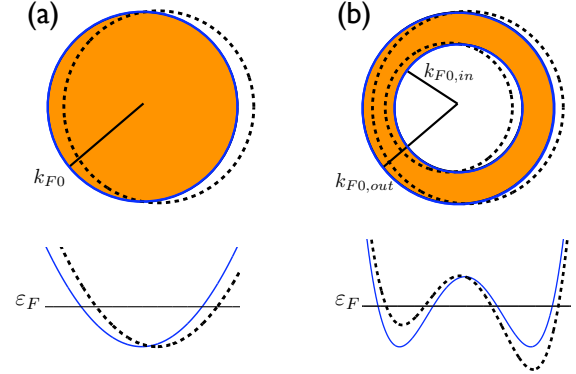


FIG. 1: (color online)  $\ell = 1$  Pomeranchuk instability of a conventional Fermi liquid and of density-unbalanced BLG. The lower panels illustrate the quasiparticle band dispersions that correspond to the Fermi surfaces illustrated in the top panels. a) The circular orange Fermi circle with Fermi radius  $k_{F0}$  denotes the occupied states of a two-dimensional Fermi sea. A Pomeranchuk instability occurs when energy is reduced by a momentum-space angle-dependent change in Fermi radius that is proportional to  $\cos(\ell\theta)$ . For  $\ell = 1$  the distorted Fermi surface, indicated here by the dashed black circle, is simply shifted in momentum space. b) The disk-shaped orange region with inner and outer Fermi radii  $k_{F0,in}$  and  $k_{F0,out}$  denotes occupied conduction band states in unbalanced BLG. Shifts in the inner and outer Fermi radii that are proportional to  $\cos(\theta)$  and have opposite signs for the inner and outer Fermi lines, thicken and thin the disk in opposite directions as indicated by the black dashed lines. The distorted state will tend to have lower interaction energy because the occupied states are more concentrated in momentum space.

a new family of materials whose electronic structure is at the same time remarkably simple and remarkably variable. Single-layer graphene is described by a massless-Dirac-fermion model with conduction and valence bands that touch at two different points in momentum space and disperse linearly over a wide energy region. In a neutral Bernal-stacked bilayer with a very strong electric field directed perpendicular to the layers [14], the Fermi level lies within the conduction band of one layer and the valence band of the other. Inter-layer hybridization with strength  $\gamma_1$  opens up an avoided crossing gap centered at a finite 2D wavevector magnitude between states localized in opposite layers, yielding an unusual semiconductor with an electrically tunable gap. Our interest here

is in the electronic properties of degenerate electrons in the conduction band (or holes in the valence band) of this density-unbalanced configuration of BLG. When angular variation of the avoided crossing gap due to trigonal warping effects is neglected [15], the conduction band minimum occurs along a circle in momentum space and the non-interacting electron Fermi surface is an annulus as indicated in Fig. 1(b). Because the band density-of-states diverges as energy approaches the conduction band minimum it is clear, as noted previously [16, 17], that interactions may play a central role in determining electronic properties and that instabilities that break symmetries are likely. The possibilities include common broken symmetries which lead to ferromagnetic or density-wave states but also, as we argue below, the spontaneous current states imagined by London, Heisenberg and others.

We illustrate our main point by considering a toy model which ignores trigonal warping and spin and valley degrees-of-freedom, and by using mean-field theory to estimate the toy model Fermi-liquid parameters. The Hartree-Fock energy functional [18] is

$$E_{\text{HF}}[\{n_{\mathbf{k}}\}] = \sum_{\mathbf{k}} [\varepsilon_{\text{b}}(k) - \mu] n_{\mathbf{k}} - \frac{1}{2A} \sum_{\mathbf{k}, \mathbf{k}'} n_{\mathbf{k}} V_{\mathbf{k}-\mathbf{k}'} n_{\mathbf{k}'} , \quad (1)$$

where  $\varepsilon_{\text{b}}(k)$  are bare-band energies, which are isotropic and thus depend only on  $k = |\mathbf{k}|$ , and  $A$  is the 2D electron system area. In our toy model we assume that the interaction  $V_{\mathbf{k}-\mathbf{k}'}$  depends only on  $|\mathbf{k} - \mathbf{k}'|$ . Expanding this energy functional in powers of the deviation  $\delta n_{\mathbf{k}}$  from the occupation numbers  $n_{\mathbf{k}}^{(0)}$  corresponding to the undistorted Fermi surface yields an energy expression of the Fermi-liquid-theory form:

$$E_{\text{HF}}[\{n_{\mathbf{k}}\}] = E_0 + \sum_{\mathbf{k}} \varepsilon_{\text{b}}^{\text{HF}}(k) \delta n_{\mathbf{k}} - \frac{1}{2A} \sum_{\mathbf{k}, \mathbf{k}'} \delta n_{\mathbf{k}} V_{\mathbf{k}-\mathbf{k}'} \delta n_{\mathbf{k}'} , \quad (2)$$

where the Hartree-Fock band energy  $\varepsilon_{\text{b}}^{\text{HF}}(k)$  is defined by

$$\varepsilon_{\text{b}}^{\text{HF}}(k) = \varepsilon_{\text{b}}(k) - \int \frac{d^2 \mathbf{k}'}{(2\pi)^2} n_{\mathbf{k}'}^{(0)} V_{\mathbf{k}-\mathbf{k}'} . \quad (3)$$

Because the total energy is sensitive to cancellations between quasiparticle-velocity renormalizations and quasiparticle-interaction corrections, we must treat the two contributions on an equal footing. Below we consider the quasiparticle-velocity renormalization first and use this analysis to define our notation.

We begin by calculating the Hartree-Fock velocities, *i.e.* the momentum-space radial derivatives of the quasiparticle energy at the outer ( $n = \text{out}$ ) and inner ( $n = \text{in}$ ) Fermi circles. The velocities are most conveniently evaluated by replacing the derivative with respect to  $\mathbf{k}$  in  $V_{\mathbf{k}-\mathbf{k}'}$  by a derivative with respect to  $\mathbf{k}'$ . When the interaction correction to the velocity is integrated by parts, this derivative then acts on  $n_{\mathbf{k}'}^{(0)}$  picking out states at the

Fermi energy. We find that

$$v_n^{\text{HF}}(k) = \text{sgn}(n) |v_n(k)| + \frac{1}{2\pi\hbar} \int_0^{2\pi} \frac{d\varphi}{2\pi} \cos(\varphi) \times \{ [k' V_{\mathbf{k}-\mathbf{k}'}]_{k'=k_{\text{F0,out}}} - [k' V_{\mathbf{k}-\mathbf{k}'}]_{k'=k_{\text{F0,in}}} \} , \quad (4)$$

where  $\phi$  is the difference between the angular coordinates of  $\mathbf{k}$  and  $\mathbf{k}'$ , and we have noted that  $V_{\mathbf{k}-\mathbf{k}'}$  depends only on  $\phi$  once  $k$  and  $k'$  are fixed [19]. This leads to

$$\frac{v_{\text{out}}^*}{v_{\text{out}}} = 1 + \alpha_{\text{out}} \left( U_{\text{out,out}}^{(1)} - \sqrt{\frac{k_{\text{F0,in}}}{k_{\text{F0,out}}}} U_{\text{out,in}}^{(1)} \right) , \quad (5)$$

where  $v_{\text{out}}^* \equiv v_{\text{out}}^{\text{HF}}(k_{\text{F0,out}})$ ,  $\alpha_{\text{out}} \equiv e^2/(\hbar v_{\text{out}})$ ,  $U_{n,n'}^{(m)} \equiv V_m(k_{\text{F0},n}, k_{\text{F0},n'}) (k_{\text{F0},n} k_{\text{F0},n'})^{1/2} / (2\pi e^2)$  is a dimensionless interaction parameter that is symmetric in the  $n, n'$  inner/outer indices, and the  $V_m$ 's are Fourier components of the interaction's  $\phi$ -dependence. The corresponding expression for  $v_{\text{in}}^*$  can be obtained by interchanging the in and out labels.

To look for Pomeranchuk instabilities we parameterize the inner ( $n = \text{in}$ ) and outer ( $n = \text{out}$ ) Fermi surfaces in terms of dimensionless distortion functions:

$$k_{\text{F},n} = k_{\text{F0},n} [1 + a_n(\theta)] \equiv k_{\text{F0},n} + \delta k_{\text{F},n}(\theta) , \quad (6)$$

and expand these in terms of their angular momentum components  $a_n(\theta) = \sum_{\ell=-\infty}^{+\infty} a_{n\ell} e^{i\ell\theta}$ . The distorted state has a  $\delta n_{\mathbf{k}}$  which is non-zero only in the vicinity of the inner and outer Fermi lines. It is easy to verify that the first-order correction to the energy vanishes. To obtain the second-order correction we linearize the Hartree-Fock energies around  $k_{\text{F0,in}}$  and  $k_{\text{F0,out}}$ :

$$\varepsilon_{\text{b}}^{\text{HF}}(k) \simeq \begin{cases} -\hbar v_{\text{in}}^* (k - k_{\text{F0,in}}) \\ \hbar v_{\text{out}}^* (k - k_{\text{F0,out}}) \end{cases}$$

and add the quasiparticle interaction contribution to obtain the energy change for small distortions:

$$\begin{aligned} \frac{E^{(2)}}{A} &= \frac{\hbar}{4\pi} \sum_{n,n'} \sum_{\ell=-\infty}^{+\infty} \left\{ v_n^* \delta_{n,n'} \right. \\ &\quad \left. - \frac{e^2}{\hbar} \text{sgn}(nn') U_{n,n'}^{(\ell)} \right\} k_{\text{F0},n}^{3/2} k_{\text{F0},n'}^{3/2} a_{n\ell} a_{n'\ell}^* . \end{aligned} \quad (7)$$

This is our principal result. Note that for a Galilean-invariant system which has only an outer Fermi radius the two interaction contributions to the  $\ell = 1$  distortion energy cancel, recovering the general result [6–8] mentioned previously. An  $\ell = 1$  Pomeranchuk instability occurs when the determinant of the following matrix

$$\begin{pmatrix} v_{\text{out}}^* - (e^2/\hbar) U_{\text{out,out}}^{(1)} & (e^2/\hbar) U_{\text{out,in}}^{(1)} \\ (e^2/\hbar) U_{\text{out,in}}^{(1)} & v_{\text{in}}^* - (e^2/\hbar) U_{\text{in,in}}^{(1)} \end{pmatrix} \quad (8)$$

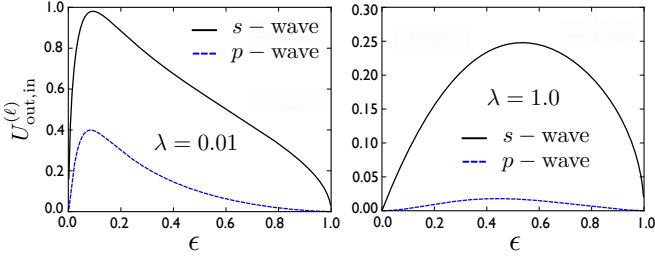


FIG. 2: (color online) The dimensionless “outer-inner” pseudopotential  $U_{\text{out,in}}^{(\ell)}$  vs.  $\epsilon = b/(2\bar{k})$  for  $\ell = 0$  ( $s$ -wave) and  $\ell = 1$  ( $p$ -wave). This plot is for  $\delta = 2/(a_{\text{eff}}\bar{k}) = 1$  where  $a_{\text{eff}}$  and  $\bar{k}$  are defined in the main text. The parameter  $b$  measures the thickness of the ring and  $b \rightarrow 0$  in the limit in which the Fermi energy  $\varepsilon_F$  equals the band-edge energy  $\epsilon_{\text{min}}$ . The left panel is for a very small screening parameter,  $\lambda = 0.01$ , while the right panel is for fully screened Thomas-Fermi interactions,  $\lambda = 1.0$ .

is zero. Using Eq. (5) (and the corresponding equation for  $v_{\text{in}}^*$ ) we finally find the following criterion:

$$1 - \left( \alpha_{\text{out}} \sqrt{\frac{k_{F0,\text{in}}}{k_{F0,\text{out}}}} + \alpha_{\text{in}} \sqrt{\frac{k_{F0,\text{out}}}{k_{F0,\text{in}}}} \right) U_{\text{out,in}}^{(1)} = 0. \quad (9)$$

Notice that this instability criterion depends only on the “outer-inner” interaction.

We estimate the disk Fermi-liquid interaction parameters using

$$V_{\mathbf{k}-\mathbf{k}'} = \frac{2\pi e^2}{|\mathbf{k} - \mathbf{k}'| + \lambda q_{\text{TF}}}, \quad (10)$$

where  $q_{\text{TF}}$  is the Thomas-Fermi screening wave vector, and  $\lambda \in [0, 1]$  is a dimensionless control parameter that allows us to interpolate between bare-Coulomb ( $\lambda = 0$ ) and Thomas-Fermi ( $\lambda = 1$ ) limits. The Thomas-Fermi screening wave vector is proportional to the density-of-states at the Fermi energy,  $N(0) = 2m_{\text{eff}}\bar{k}/(\pi\hbar^2b)$  where  $b = k_{F0,\text{out}} - k_{F0,\text{in}}$ ,  $\bar{k} = (k_{F0,\text{out}} + k_{F0,\text{in}})/2$ , and  $m_{\text{eff}}$  parameterize the band-energy dispersion at its minimum. It follows that  $q_{\text{TF}} = 2\pi e^2 N(0) = 4\bar{k}/(a_{\text{eff}}b)$  where  $a_{\text{eff}} = \hbar^2/(m_{\text{eff}}e^2)$  is an effective Bohr radius. The inner-outer interaction parameters  $U_{\text{out,in}}^{(\ell)}$  obtained using this approximation depend on two dimensionless quantities,  $\epsilon = b/(2\bar{k})$  and  $\delta = 2/(a_{\text{eff}}\bar{k})$ , and are plotted for  $\ell = 0, 1$  in Fig. 2. The strong declines for small  $\epsilon$  are due to strong Thomas-Fermi screening and are certainly an artifact of this approximation in combination with the divergent Fermi-level density-of-states for  $\epsilon \rightarrow 0$ . We can make two conclusions based on these estimates: i) Interactions in the  $\ell = 1$  channel are strong enough to produce an  $\ell = 1$  Pomeranchuk instability and ii) Interactions in the  $\ell = 0$  channel are likely even stronger than those in the  $\ell = 1$  channel. If bilayer graphene had a single valley,  $\ell = 0$  instabilities, which imply phase separation into low and high density regions, would be forbidden by the

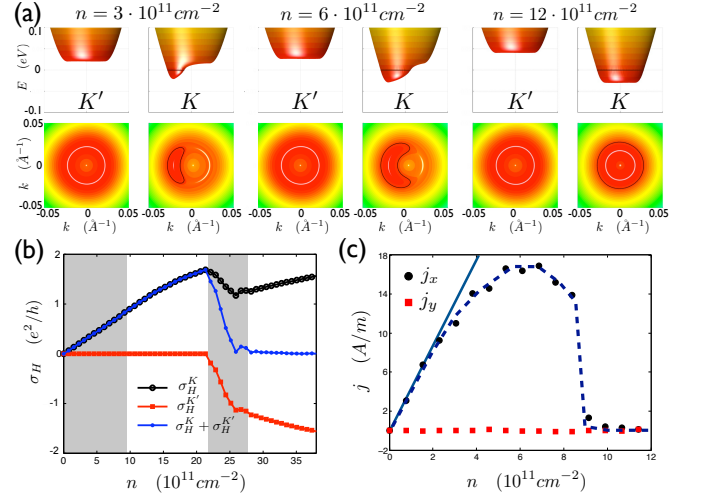


FIG. 3: (color online) Quasiparticle bands, Hall conductivities and spontaneous currents due to  $\ell = 0$  and  $\ell = 1$  Pomeranchuk instabilities in unbalanced BLG. These results were obtained with an external potential difference corresponding to a perpendicular electric field of 1 V/nm between layers. (a) Valley polarized quasiparticle bands for three different total carrier densities (both spins). The upper and lower panels illustrate conduction band energy dispersions and constant energy contours respectively. The left and right columns are for momenta near the  $K'$  and  $K$  valleys. The  $\ell = 0$  instability is signaled by unequal occupation of the two valleys. The  $\ell = 1$  instability is signaled by the breaking of rotational symmetry within an occupied valley. The solid black line marks the position of the Fermi level which is chosen as the zero of energy:  $\varepsilon_F = 0$ . (b) Spontaneous Hall effect vs. carrier density. The Hall effect [Eq. (11)] reflects spontaneous valley polarization. We find that the Hall conductivity increases monotonically with carrier density until minority ( $K'$ ) valley with opposite Hall conductivity starts to be occupied. The shaded regions indicate intervals of carrier density over which spontaneous currents occur due to  $\ell = 1$  Pomeranchuk instabilities. The lower density instability occurs within the majority valley and the higher density instability within the minority valley. (c) Total spontaneous persistent current evaluated from Eq. (12) for both spins. The conduction and valence bands of the polarized valley have similar contributions to the total persistent current. For this calculation we used a  $k$ -point sampling density near the Dirac cones equivalent to a density of  $4608 \times 4608$  points in the whole Brillouin zone. The blue dotted line represents a guide to the eye for the numerical data points. The slope of the continuous line indicates the effective quasiparticle velocity of the current carrying states, which is about 1.5% of the Fermi velocity in graphene.

long-range Coulomb interaction. However, because of the presence of valley and spin degrees of freedom it appears that the strongest instabilities of the normal state will have  $\ell = 0$ , leading to spin [16] or valley polarized states.  $\ell = 1$  Pomeranchuk instabilities do however appear possible within these polarized states.

We have corroborated the conclusions drawn from our toy-model calculation by performing self-consistent  $\pi$ -

orbital lattice Hartree-Fock calculations similar to those described in Ref. 20. For these calculations we added interactions to a band model with nearest-neighbor intra-layer hopping  $\gamma_0 = 3.12$  eV and inter-layer hopping  $\gamma_1 = 0.377$  eV, ignoring other hopping parameters for the sake of simplicity [21]. We have suppressed spin-polarization instabilities in these calculation so that  $\ell = 0$  instabilities are manifested by valley rather than spin-polarization. Because external electric fields in unbalanced BLG lead to large Berry curvatures  $\Omega_{n,\mathbf{k}}$  of opposite sign in the vicinity of  $K$  and  $K'$  valley points [22] the anomalous Hall conductivity can be used as an observable for spontaneous valley polarization. The Hall conductivity (per spin) is calculated by integrating  $\Omega_{n,\mathbf{k}}$  over occupied quasiparticle states near the Dirac points,

$$\sigma_H = \frac{e^2}{\hbar} \int \frac{d^2\mathbf{k}}{(2\pi)^2} \sum_n f_{n,\mathbf{k}} \Omega_{n,\mathbf{k}}, \quad (11)$$

where  $f_{n,\mathbf{k}}$  is the Fermi-Dirac distribution and a sum is carried over the band index  $n$ .

To evaluate the spontaneous current density associated with the  $\ell = 1$  instability we use the current density operator  $\mathbf{j} = -e\nabla_{\mathbf{k}}\mathcal{H}_0/(A\hbar)$ . Because the interaction Hamiltonian is independent of position, the current operator is given by its non-interacting one-body form, which is diagonal in Bloch momentum. Its expectation value (per spin) in the mean-field state is therefore

$$\langle \mathbf{j} \rangle = \frac{-e}{A\hbar} \sum_{\mathbf{k},n} f_{n,\mathbf{k}} \langle \varphi_{n,\mathbf{k}} | \nabla_{\mathbf{k}} \mathcal{H}_0 | \varphi_{n,\mathbf{k}} \rangle, \quad (12)$$

where  $|\varphi_{n,\mathbf{k}}\rangle$  are the Hartree-Fock single-particle states. We evaluate the current density averaging the numerical derivative of the tight-binding Hamiltonian in momentum space. Fig. 3 plots Hall conductivities and spontaneous currents evaluated for this model which demonstrate that spontaneous valley polarization occurs for carrier densities smaller than  $\sim 25 \times 10^{11} \text{ cm}^{-2}$ , and spontaneous currents for carrier densities smaller than  $\sim 9 \times 10^{11} \text{ cm}^{-2}$  and again near the onset of minority valley occupation. These mean-field calculations likely overestimate the density-ranges over which the broken symmetry states occur.

Because they appear only at low carrier densities, comparable to or smaller than typical disorder-induced density-fluctuation scales for bilayer samples on silicon oxide substrates, and because large electric fields are favorable for their occurrence, we anticipate that momentum space condensation is at present most likely to occur in dual-gated bilayer graphene samples on h-BN substrates [23]. We expect that trigonal warping of the unbalanced bilayer conduction bands will favor momentum space condensation over competing [17] density-wave instabilities. Because the  $\ell = 1$  Pomeranchuk instability is likely only within states in which spin or valley polarization, or both, has already occurred, its appearance

should be signaled most clearly by observables that reflect broken inversion symmetry, rather than simply broken time reversal symmetry. Since spontaneous currents cannot flow in closed samples, or even in samples that are in contact with an unbiased external circuit, equilibrium momentum space condensation must be accompanied by domain formation. We expect that this property will lead, not to dissipationless current flow of the type observed in superconducting samples, but instead to highly non-linear and hysteretic current-voltage characteristics.

Heisenberg and London imagined that momentum-space condensation might explain superconductivity. If spontaneous current states do occur in unbalanced bilayer graphene, it will be fascinating to sort out the similarities and differences between the properties of these broken symmetry states and those of superconductors.

*Acknowledgments.* Financial support was received from Welch Foundation grant TBF1473, from NRI-SWAN, and from DOE Division of Materials Sciences and Engineering grant DE-FG03-02ER45958.

- 
- [1] J. Bardeen, L.N. Cooper, and J.R. Schrieffer, Phys. Rev. **106**, 162 (1957).
  - [2] W. Heisenberg, Zeits. f. Naturforschg. **32**, 65 (1948).
  - [3] M. Born and K.C. Cheng, Nature **161**, 1017 (1948).
  - [4] F. London, Phys. Rev. **74**, 562 (1948).
  - [5] I.J. Pomeranchuk, Sov. Phys. JETP **8**, 361 (1958).
  - [6] D. Bohm, Phys. Rev. **75**, 502 (1949).
  - [7] H.G. Smith and J.O. Wilhelm, Rev. Mod. Phys. **7**, 266 (1935).
  - [8] G.F. Giuliani and G. Vignale, *Quantum Theory of the Electron Liquid* (Cambridge University Press, Cambridge, 2005).
  - [9] J. Quintanilla and A.J. Schofield, Phys. Rev. B **74**, 115126 (2006).
  - [10] C.J. Halboth and W. Metzner, Phys. Rev. Lett. **85**, 5162 (2000).
  - [11] E. Fradkin *et al.*, Annu. Rev. Condens. Matt. Phys. **1**, 153 (2010).
  - [12] Pomeranchuk instabilities have been discussed in the context of single-layer graphene at extremely high doping: B. Valenzuela and M.A.H. Vozmediano, New J. Phys. **10**, 113009 (2008).
  - [13] A.K. Geim and A.H. MacDonald, Phys. Today **60**(8), 35 (2007); A.H. Castro Neto *et al.*, Rev. Mod. Phys. **81**, 109 (2009).
  - [14] E.V. Castro *et al.*, J. Phys.: Condens. Matter **22**, 175503 (2010).
  - [15] E. McCann and V.I. Fal'ko, Phys. Rev. Lett. **96**, 086805 (2006).
  - [16] T. Stauber *et al.*, Phys. Rev. B **75**, 115425 (2007); E.V. Castro *et al.*, Phys. Rev. Lett. **100**, 186803 (2008); V.S. Kusminskiy, D.K. Campbell, and A.H. Castro Neto, Europhys. Lett. **85**, 58005 (2009).
  - [17] Another state that might occur in doped bilayer graphene or in electronic systems with similar electronic structure (*e.g.* a low-density 2D electron gas with Rashba spin-orbit coupling) is a charge-density-wave state. See,

- for example, E. Berg, M.S. Rudner, and S.A. Kivelson, arXiv:1108.1222 and K. Yang and S. Sachdev, Phys. Rev. Lett. **96**, 187001 (2006).
- [18] This expression ignores the Hartree energy and is therefore valid only for uniform electron density states.
  - [19] G. Borghi *et al.*, Solid State Commun. **149**, 1117 (2009).
  - [20] J. Jung *et al.*, Phys. Rev. B **83**, 115408 (2011); Phys. Rev. B **84**, 085446 (2011).
  - [21] While similar instabilities are also found when additional hopping terms are considered, we have chosen the simplest nearest-neighbor model to illustrate more clearly the essence of the physics that underlies the instability.
  - [22] D. Xiao, W. Yao, and Q. Niu, Phys. Rev. Lett. **99**, 236809 (2007).
  - [23] C.R. Dean *et al.*, Nature Nanotech. **5**, 722 (2010).